

# A Double Vacuum Window Mechanism for Space-borne Applications

K. Zilic,<sup>1</sup> A. Aboobaker,<sup>2</sup> F. Aubin,<sup>1</sup> C. Geach,<sup>1</sup> S. Hanany,<sup>1</sup> N. Jarosik,<sup>3</sup> M. Milligan,<sup>1</sup> and I. Sagiv<sup>1</sup>

<sup>1)</sup>*University of Minnesota/Twin Cities, School of Physics and Astronomy, 116 Church St, Minneapolis, MN 55455, USA*

<sup>2)</sup>*Jet Propulsion Laboratory, 4800 Oak Grove Dr, Pasadena, CA 91011, USA*

<sup>3)</sup>*Department of Physics, Princeton University, Princeton, NJ 08544, USA*

(Dated: 2 November 2021)

We present a vacuum window mechanism that is useful for applications requiring two different vacuum windows in series, with one of them movable and resealable. Such applications include space borne instruments that can benefit from a thin vacuum window at low ambient pressures, but must also have an optically open aperture at atmospheric pressures. We describe the implementation and successful operation with the EBEX balloon-borne payload, a millimeter-wave instrument designed to measure the polarization of the cosmic microwave background radiation.

PACS numbers: 07.30.-t, 07.30.Kf, 42.79.Ag, 07.57.-c, 98.80.Es, 42.88.+h

Keywords: Vacuum window, Millimeter waves, Atmospheric conditions

## I. INTRODUCTION

The use of vacuum windows is ubiquitous throughout science and engineering. In certain applications there is a need to implement two vacuum windows in series. Examples include balloon-borne or space-based applications in which one prefers to use a thicker window for the larger differential pressure on the ground, and a thinner window when the payload is above Earth's atmosphere. If the experiment is to be reusable, the vacuum window mechanism must be reversible, that is, the atmospheric pressure seal must be resealable.

Ground testing and calibration of experiments that are sensitive to electromagnetic radiation require that both vacuum windows in the series be transparent to the desired wavelengths. The choice of vacuum window material depends, among other factors, on the wavelength of use. Many such applications require windows with low loss, low reflection, and low emission. Useful materials in the millimeter wavelength include polyethylene and polypropylene. They are readily available in a large range of thicknesses and sizes, and have low cost. They have relatively low index of refraction, making the fabrication of anti-reflection coating less of a challenge compared to higher index materials. Ultra high molecular weight polyethylene (UHMWPE) and polypropylene have loss tangents of  $8 \times 10^{-5}$  and  $4 \times 10^{-4}$ , respectively, among the lowest at this waveband<sup>2,5</sup>.

In this paper we describe a vacuum window that we developed for the balloon-borne E and B Experiment (EBEX). It consisted of two polyethylene vacuum windows in series, one of them removable and resealable. We call the apparatus the double window mechanism (DWM). In Section II we describe the requirements that led to the development of the DWM; and in Section III we discuss the specifics of the design of the DWM as well as the testing performed on the DWM and the results found.

## II. EBEX

E and B Experiment (EBEX) was a stratospheric balloon-borne experiment designed to measure the polarization of the cosmic microwave background radiation<sup>8,9</sup>. It consisted of an ambient temperature telescope focusing light into a cryogenic receiver. The receiver had

an array of nearly a thousand bolometric transition edge sensors operating at a temperature of 0.25 K. The experiment had three frequency bands centered on 150, 250 and 410 GHz and collected data in a flight circumnavigating Antarctica in January 2013.

The optical design determined the 300 mm open diameter of the receiver’s vacuum window. Below the window we placed reflective filters to reject high frequency radiation. Space constraints dictated that these filters be placed no farther than 10 mm below the vacuum window, limiting the maximum bowing acceptable for the window material before damaging the filters.

We considered several materials for the vacuum window including alumina, silicon, sapphire, Zotefoam, polypropylene, and varieties of polyethylene. We chose ultra high molecular weight polyethylene (UHMWPE) because it has low loss, a relatively low index and our collaborators had already developed a broad-band anti-reflection coating for it; because it is not fragile; and because it is readily available at many sizes and thicknesses.

We measured the central deflection of 300 mm diameter UHMWPE window under atmospheric differential pressure for a number of thicknesses. We found that a minimum of 12.7 mm thick material was needed to provide a deflection of less than 10 mm. Although total absorption with this thickness is only 0.5%, 1.1%, and 3.0%, at the three EBEX frequency bands, the emission of such a room temperature window would have represented 8%, 11%, and 14% of the total optical load absorbed by the detectors at 150, 250, and 410 GHz, respectively. The temperature at float altitude is close to room temperature. To make the optical load and resultant photon noise from the window negligible compared to other sources, we decided to use two windows in series: a removable thick window for ground operations, and, below it, a thinner window only for float altitude. A comparison between the optical load for the two thicknesses is given in Table I. We use the words ‘above’ and ‘below’ to indicate relative positions closer to the higher and lower pressures, respectively.

Band	12.7 mm window	1 mm window
150 GHz	8 %	0.1 %
250 GHz	11 %	1 %
410 GHz	14 %	1 %

TABLE I. Calculated fractional in-band optical loading on the EBEX detectors due to a single window of either 12.7 mm or 1 mm thickness in the optical path.

### III. DOUBLE WINDOW DESIGN

#### A. Overview

The DWM consisted of a permanent 1 mm UHMWPE, anti-reflection coated window, which we call the ‘thin window’. On the ambient pressure side of the thin window we placed a movable plate with two apertures. One 300 mm aperture had a 12.7 mm thick UHMWPE, anti-reflection coated ‘thick window’; the other 380 mm aperture was open. Figure 1 shows a cross-section of the construction and Figure 2 shows a solid model of the entire apparatus. A copper tube with a valve connected the receiver cavity to the volume immediately above

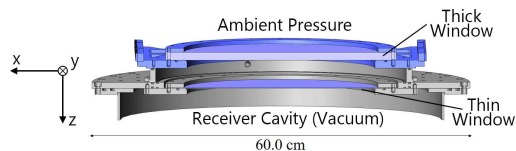


FIG. 1. Cross-section view of the DWM. The thick window was movable in the y direction, exposing an open aperture above the thin window (see Figure 2). It was also resealable. The cavity between the windows was connected with a tube and valve (not shown) to the receiver cavity.

the thin window. On the ground the thick window was always positioned above the thinner one. When the receiver was evacuated we also evacuated the chamber between the two windows. Before the payload was launched we closed the valve connecting the receiver and intra-window cavity. When the payload reached float altitude we actuated a motor to move the two-aperture plate and place the open aperture in position above the thin window. Before flight termination the motor was actuated again to move the thick window back into its ground-operations position.

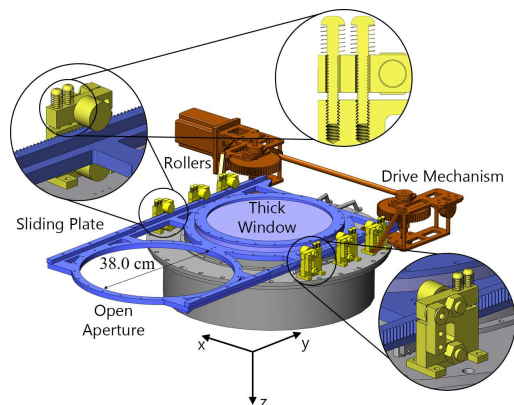


FIG. 2. Model of the DWM assembly. It consisted of a plate with two apertures (blue), a drive mechanism (brown), and six spring-loaded rollers, each with two springs (yellow). The mechanism gave the capability to either have the thick window seal the receiver, the configuration shown, or move the sliding plate in the  $+y$  direction and replace the thick window with an open aperture.

## B. Thin Window

The 3636 kg total suspended weight below the 963,000 m<sup>3</sup> helium balloon gave high likelihood for flight altitude above 33 km and therefore an ambient pressure below  $\sim 6$  torr. Figure 3 shows our measurement of the central deflection of a 300 mm UHMWPE window as a function of window thickness for several differential pressures of 4 torr and above. The differential pressures span equivalent altitudes between 29 and 35 km<sup>1</sup>. We chose a thickness of 1 mm because it gave negligible additional emission, and even at altitude as low as 28 km its maximum deflection was only 3 mm, giving ample space margin from the infrared filters below it. Two flat aluminum rings with inside (outside) diameter of 310 (368) mm were glued to the top and bottom of the thin window with Miller Stephenson Epoxy 907 and bolted against an o-ring situated in a standard o-ring groove.

## C. Movable, Resealable Window

The DWM mechanism had two main elements: motion and seal. (We followed a design similar to one initially implemented by the XPER experiment<sup>7</sup>.)

The motion part of the DWM consisted of a stepper motor driving a horizontal shaft with two worms, one on either side of the moving plate; see Figure 4. The worms coupled to worm gears on two vertical shafts that also had spur gears. The spur gears coupled to racks mounted on either side of the moving plate. The plate rode between 6 pairs of 300-grade stainless steel rollers, 3 pairs on each side of the plate.

A gear system was used due to its simplicity, compactness, and high output torque, as well as tolerance for low-temperatures, such as may be experienced during the ascend period of flight with temperatures down to  $-50^{\circ}\text{C}$ . The rack was mounted on the sides of the sliding plate, rather than on top or bottom, because the seal/reseal function was provided through

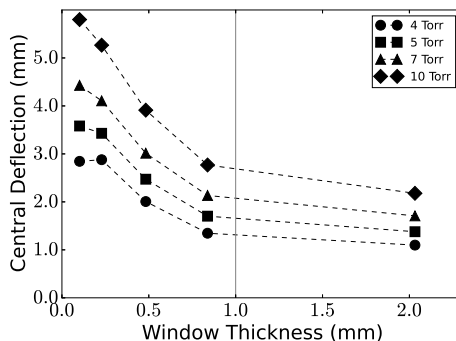


FIG. 3. Central deflection versus window thickness for different pressure differentials. A 1.0 mm window was chosen.

motion in the  $z$  direction (see Figures 1 and 2). We used two symmetric spur gear and worm/worm gear systems on either side of the sliding plate to ensure proper movement. One of the worm/worm gear systems was right-handed and the other was left-handed due to the mirror symmetry of the sliding plate.

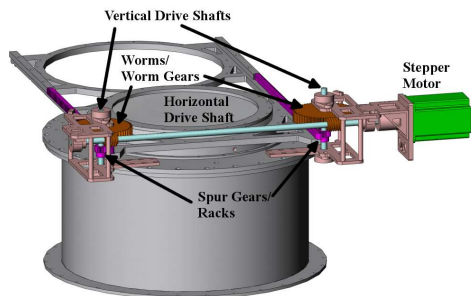


FIG. 4. The DWM drive mechanism consisted of a stepper motor (green) driving a horizontal shaft drive shafts (cyan) with two worm/worm gears (brown), coupling to two vertical shafts (cyan) with two spur gear/racks (magenta).

The thick window was permanently clamped directly onto a Buna-N o-ring on the movable plate. We also used an o-ring to facilitate the seal between the moving plate and the stationary surface of the DWM; both were made of aluminum. A relatively high hardness, Shore A 75, Buna-N o-ring was mounted onto the stationary surface. The movable vacuum seal required two functions, sealing in fixed known locations, and sliding between these locations without damaging the o-ring. Importantly, no vacuum sealing function was required during the motion. To achieve these functions we provided for a small  $z$  displacements of the moving plate by means of triangular notches on the bottom side of the moving plate; see Figure 5. The position of the slots matched the positions of the bottom rollers in seal positions. In these positions the effectively thinner plate would move down and seal against the o-ring. Sealing force was provided by springs that forced the top rollers in the direction of the bottom rollers. During motions, the plate rolled out of the notches against the force of the springs, thus moving away from the o-ring seal.

The triangular notches in the sliding plate made an angle of  $26.7^\circ$  relative to the track face and were 3.3 mm deep. The geometry of the notches was chosen to give clearance for the sliding plate to travel above the o-ring when moving and to compress the o-ring when the 25.4 mm diameter rollers were seated in the notches. The o-ring was seated in a dovetail groove which set its maximum linear compression to be 0.71 mm, 20% of the 3.53 mm diameter. This compression and the o-ring hardness required a compressive force

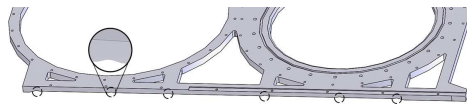


FIG. 5. The DWM sliding plate with triangular notches highlighted on the bottom surface.

per length of 1.2 to 6.6 N/mm for proper vacuum sealing and o-ring durability<sup>6</sup>. We chose a value of 2.9 N/mm, and with the 410 mm nominal diameter o-ring, this gave a total required compressive force of 3700 N. In a ground configuration, a force of 13300 N was exerted uniformly on the o-ring due to the pressure differential across the thick window; however, at float altitude, the pressure differential drops, providing only 180 N of force. Furthermore, upon resealing at the end of flight, there is no pressure differential across the thick window at all. To provide the required force during flight, 12 springs with spring constant of 41.3 N/mm were compressed 7.5 mm each by engaging the compression screws by hand, which then pressed on the sliding plate and o-ring via the rollers located above the sliding plate; see Figure 2.

We calculated that a force of 2300 N was required to move the rollers out of the notches. Given the radius of the spur gears of 12.7 mm and the 60:1 worm/worm gear ratio, this required a minimum motor torque of 0.49 Nm. However, worm/worm gear efficiency depends on the coefficient of friction between the two surfaces as,

$$\text{Efficiency} = \tan \gamma \frac{1 - \mu \tan \gamma}{\mu + \tan \gamma} \quad (1)$$

where  $\gamma = 4.8^\circ$  was the worm lead angle<sup>3</sup>. We assumed that the kinetic coefficient of friction  $\mu$  between the cast iron worm gear and steel worm was 0.2<sup>4</sup> when unlubricated, which gives an efficiency of 29%. In this case the minimum required torque is 1.69 Nm. We used Dow Corning Molykote dry lubricant to decrease the friction between the components and protect the open gearing from oxidation. With the dry lubricant we expected a coefficient of friction between 0.02 and 0.06<sup>4</sup>, and thus an increase in the worm/worm gear efficiency to between 58% and 81%, and a reduction in the required motor torque to between 0.84 and 0.60 Nm, respectively. A stepper motor with a stall torque of 3.88 Nm (Kollmorgen model M093-LE14) was chosen to give more than a factor of two safety for the unlubricated case.

The DWM was operated at low speeds, taking 3.3 minutes to move the 419 mm from the thick window to open aperture states. At this speed the stepper motor operated in its high-torque regime. Since the DWM was operated only twice during flight, its operation time had negligible effect on total observation time. We monitored the position of the sliding plate with two electrical limit switches that were located at either end of the travel and were depressed when the sliding plate was in the thick window or open aperture positions. The state of these switches were continuously read out as analog voltages.

Aluminum components were used extensively and all steel components were lightweighted. In total, the DWM had a mass of 22 kg, including the windows, vacuum valve, bellows, and stepper motor. Military specification Buna-N o-rings rated to  $-54^\circ\text{C}$  were used for their thermal properties and abrasion durability.

#### IV. TESTING AND IN-FLIGHT OPERATION

We tested the DWM in vacuum and flight-like temperatures in an environmental chamber at the Columbia Scientific Balloon Facility in Palestine, TX. Tests were conducted twice, once in the summer of 2011 and again in the summer of 2012. For testing purposes the DWM was mounted on a fixture that simulated the receiver vacuum. We monitored the intra-window cavity pressure to check the integrity of the thick window's vacuum seal and reseal. We placed temperature sensors on several key components of the DWM including

the stepper motor, sliding plate, and the plate that simulated the receiver, and we had an ambient chamber temperature sensor. We also readout the position switches and chamber pressure continuously.

The simulated receiver and intra-window cavities were evacuated to a pressure of few torr when the apparatus was outside the environmental chamber. The valve connecting the two cavities was closed to separate them, as would be done pre-flight. The DWM testing apparatus was then placed in the chamber. The chamber was cooled to approximately  $-45^{\circ}\text{C}$ , which is near the temperature experienced during initial ascent of the payload. The chamber and DWM were then allowed to warm up and the following cycle was tested 6 and 10 times for the two testing periods, respectively: pump the chamber down to between 2 and 10 torr of pressure, move the sliding plate to the open aperture position, move the sliding plate to the thick window position, and backfill the chamber to  $\sim 100$  torr with  $\text{N}_2$  gas. The data showed robust motion of the moving plate throughout the necessary range. It also showed proper resealing of the intra-window cavity.

EBEX was launched from the balloon Facility at McMurdo Station in Antarctica at 00:30 GMT December 29, 2012. The payload achieved an altitude of approximately 36 km about 5 hours later. The payload was science operational until 06:00 GMT January 9, 2013, for a duration of 10.83 days, at which point the liquid helium cryogen expired.

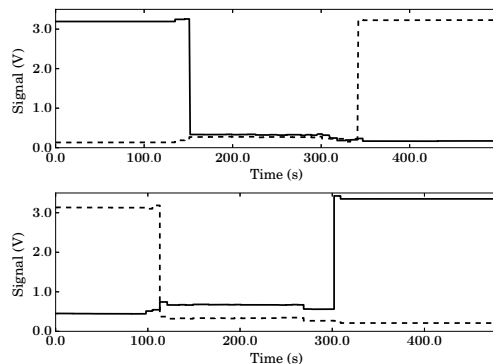


FIG. 6. DWM position encoders' signals during opening (upper) and closing (lower). High voltage indicates 'true' for the closed (solid) and open (dash) signals.

We operated the DWM twice during the flight. Three hours after launch at an altitude of 36.6 km and DWM temperature of  $15^{\circ}\text{C}$  we removed the thick window. The second time was approximately two hours after liquid helium expired at an altitude of 36.4 km and DWM temperature of  $39^{\circ}\text{C}$  when we repositioned the thick window above the thin in preparation for flight termination. The position encoder signals during these times are shown in Figure 6. These monitors indicate proper opening and closing the window. Visual inspection post-flight showed the thick window in nominal position above the thin window. Both windows and the fragile filters below them were recovered intact post-flight indicating that there was no major leak by the thick window either before it was opened or after it was resealed. Had there been a major leak, the thin window would have ruptured, or bowed sufficiently to tear the filters mounted below it. Nominal cryogenic operation of the receiver through flight and the fact that liquid helium hold time was commensurate with pre-flight predictions indicated nominal gas pressure inside the cryostat and therefore the absence of gas leaks through the thin window. We conclude that the DWM performed successfully.

## ACKNOWLEDGMENTS

Support for the development and flight of the EBEX instrument was provided by NASA grants NNX12AD50G, NNX13AE49G, NNX08AG40G, and NNG05GE62G, and by NSF

grants AST-0705134, and ANT-0944513. Zilic acknowledges support by the Minnesota Space Grant Consortium. We are grateful to Suzanne Staggs for providing the original XPER window upon which our design was based. We thank Xin Zhi Tan for help with figures.

- <sup>1</sup>US Standard Atmosphere, 1976. Technical Report TR R-408, National Oceanic and Atmospheric Administration, October 1976.
- <sup>2</sup>P.A.R. Ade and C. Tucker. Private Communication.
- <sup>3</sup>Boston Gear. *Boston Gear catalog*, 2004.
- <sup>4</sup>A. Demell. Coefficient of friction summary. [http://www-eng.lbl.gov/~ajdemell/coefficients\\_of\\_friction.html](http://www-eng.lbl.gov/~ajdemell/coefficients_of_friction.html).
- <sup>5</sup>J. W. Lamb. Miscellaneous data on materials for millimetre and submillimetre optics. *Int. J. IR and Millimeter Waves*, 17:1997–2034, 1996.
- <sup>6</sup>Parker. *Parker O-Ring Handbook*, 2007.
- <sup>7</sup>S. T. Staggs, N. C. Jarosik, S. S. Meyer, and D. T. Wilkinson. An Absolute Measurement of the Cosmic Microwave Background Radiation Temperature at 10.7 GHz. *ApJLett*, 473:L1, December 1996.
- <sup>8</sup>The EBEX Collaboration, A. Aboobaker, P. Ade, D. Araujo, F. Aubin, C. Baccigalupi, C. Bao, D. Chapman, J. Didier, M. Dobbs, W. Grainger, S. Hanany, K. Helson, S. Hillbrand, J. Hubmayr, A. Jaffe, B. Johnson, T. Jones, J. Klein, A. Korotkov, A. Lee, L. Levinson, M. Limon, K. MacDermid, A. D. Miller, M. Milligan, L. Moncelsi, E. Pascale, K. Raach, B. Reichborn-Kjennerud, I. Sagiv, C. Tucker, G. S. Tucker, B. Westbrook, K. Young, and K. Zilic. The EBEX Balloon-Borne Experiment - Gondola, Attitude Control, and Control Software. *ApJS*Supp, in print, ArXiv/1702.07020.
- <sup>9</sup>The EBEX Collaboration, A. M. Aboobaker, P. Ade, D. Araujo, F. Aubin, C. Baccigalupi, C. Bao, D. Chapman, J. Didier, M. Dobbs, C. Geach, W. Grainger, S. Hanany, K. Helson, S. Hillbrand, J. Hubmayr, A. Jaffe, B. Johnson, T. Jones, J. Klein, A. Korotkov, A. Lee, L. Levinson, M. Limon, K. MacDermid, T. Matsumura, A. D. Miller, M. Milligan, K. Raach, B. Reichborn-Kjennerud, I. Sagiv, G. Savini, L. Spencer, C. Tucker, G. S. Tucker, B. Westbrook, K. Young, and K. Zilic. The EBEX Balloon Borne Experiment - Optics, Receiver, and Polarimetry. *ApJS*, to be submitted, arXiv/1703.03847.